Micro-scale landslide displacements detection using Bayesian methods applied to GNSS data

F. Pirotti[1], A. Guarnieri[1], A. Masiero[1], C. Gregoretti[2], M. Degetto[2], A. Vettore[1]

[1] CIRGEO-Interdepartment Research Center of Geomatics, University of Padova, Italy.

(francesco.pirotti, alberto.guarnieri, andrea.masiero, antonio.vettore)@unipd.it

[2] TESAF-Department of Land, Environment, Agriculture and Forestry, University of Padova, Italy

(carlo.gregoretti, massimo.degetto)@unipd.it

Corresponding author:

F. Pirotti

CIRGEO-Interdepartment Research Center of Geomatics, University of Padova, Italy

e-mail: francesco.pirotti@unipd.it

Abstract

In this Chapter, we evaluate the movement of 6 points near a landslide body, which were surveyed with GNSS receivers over time. We apply Bayesian inference to identify the areas on the ground with statistically significant vertical (downwards) shifts. Traditional statistical methods work well only when point displacements between different survey epochs are sufficiently large compared to the standard deviations of related coordinates. In such cases, coordinate differences of some points can be marked as potential displacements. The Bayesian analysis can help to improve discrimination when height differences, computed with respect to the first measurement epoch, are at the same order of magnitude as the uncertainties of the measures. After the application of the classical statistical test, one network point, close to the upper part of the landslide area, seemed to be more unstable than the rest. In order to remove or validate the hypothesis of instability the Bayesian statistical inference was applied and all three of the upper group of points show significant shift, depending on the data *prior* parameters. This application shows that the Bayesian approach can be considered as an integration to

classical statistical significance testing (e.g., z-test), reliably showing significance in vertical directional (i.e., downward) coordinate shifts, thus detecting smaller movements.

1. Introduction

1.1 Geodetic techniques for change detection of the Earth surface

There are various techniques to monitor movements of the earth surface. Movement, by definition, has a spatial and a temporal component; two aspects which have to be measured accurately to successfully carry out tasks related to monitoring these in these two domains. Besides traditional geodetic and geotechnical surveying methods (GPS, robotic thoedolites, boreholes, inclinometers, etc.) adopted for investigation and monitoring of landslides, the use of modern remote sensing techniques for the study of these phenomena has exponentially grown in last years. The spatial component can be measured directly using classical topographic techniques, or indirectly by estimating movement using remote sensing and related geomatic techniques, i.e., photogrammetry, see Scaioni et al. (2014). The advantages of the latter methods are evident especially when one considers the low degree of accessibility of landslide areas and the high degree of risk for personnel that carries out the direct measurements. The disadvantages are related to the resolution, accuracy and capability of the sensors; for example if vegetation is present over the area, photogrammetry alone will not provide ground information, whereas *light detection and ranging* (LiDAR) allows a certain penetration of the canopy thus returns the information on the ground plane (Pirotti et al. 2013). Indeed, the possibility of acquiring highly detailed and accurate digital terrain models (DTMs) offered by *ground based interferometric synthetic aperture radar* (GBSAR, see Monserrat et al 2014) and LiDAR techniques (Dowman 2004), has opened new way of applications for the study of landslide phenomena (Lingua et al. 2007). In this field, GBSAR-based systems are mainly used for the detection and quantification of small displacements over large areas (Crosetto et al. 2014; Monserrat et al. 2014; Refice et al. 2000; Ye et al. 2004). Specific case studies regarding *synthetic aperture radar and permanent scatterers* have been tested in (Farina et al. 2006; Frangioni et al. 2014). *GNSS*

techniques with 'low-cost' receivers have been investigated and have attracted interest, for understandable economic reasons (Cina & Piras 2014). Forlani et al. (2013) use *GNSS for camera positions in the 'Photo-GNSS'* technique which applies dense-matching algorithms to retrieve surface models of the terrain, see Previtali et al. (2014) and Remondino et al. (2014). A *spatial sensor network* (SSN) was tested in Scaioni et al. (2014) including photogrammetry and contact geotechnical sensors on a scaled-down model of a landslide simulation platform. *Terrestrial laser scanners* are also becoming popular for multi-temporal change detection of landslides since Bitelli et al. (2004) especially considering that latest models have increased range and decreased weight of the sensor, and the aforementioned capability to filter out vegetation (Pirotti et al. 2013). Other references are given in Barbarella et al. 2013; 2014; Jaboyedoff et al. (2012).

All the methods mentioned are valid, and carry intrinsic pros and cons, hence have to be carefully applied depending on the characteristics of the phenomenon which is being studied, i.e., the landslide. A state of the art network of GNSS receivers remains a most robust approach to detect micro-scale displacements.

1.2 GNSS for deformation monitoring of earth surface

Geodetic techniques are widely used for monitoring the deformation of the Earth surface at different spatial and temporal scales. The term Global Navigation Satellite System (GNSS) is used to define positioning systems based on a constellation of satellites, which emit carrier signals used for defining time and position of the receiving station. Various systems are either operational or about to be so. The most recognized, due to longer operation time, is the United States' GPS constellation followed by Russia's GLONASS, Europe's Galileo, and the Chinese Beidou, see Hofmann-Wellenhof et al. (2007). Precise positioning is fundamental for monitoring dynamics of elements on the earth and to support other geo-spatial technologies, e.g., remote sensing and geographic information systems (GIS) which together act in synergy for the assessment of natural hazards and risk, see Manfré et al. (2012). GNSS estimates of position and derivatives (i.e., velocity and acceleration) are becoming

more reliable, and advanced data analysis techniques are helpful for the recognition of features in the GNSS time-series, e.g., non linear behaviours, discontinuities in the signal and in its derivatives. Detection of signal discontinuities between two or more GNSS multi-temporal surveys, or in a whole time-series, can be accomplished through the use of advanced analysis techniques such as *wavelets*, the *Bayesian*, and the *variational methods*, see Borghi et al. (2012). Discontinuities which are expected to be very small and compatible with the signal noise motivate the use of advanced data analysis techniques to investigate significant modifications of point positions, see Betti et al. (1999). The ability to detect GNSS points whose movement can be considered significantly different from noise and other factors not related to the phenomenon of interest, is an important step in the field of geomatics applied to natural hazards and risk. Investigations in this sense have been carried out also by (Wang & Soler 2012) where a GNSS dense network was monitored to detect a creeping landslide in a two year period; authors also discuss influence of rainfall events which degrade performance of the receivers. The Bayesian approach in structuring a significance test (Koch 2007) on the displacement of point position is a robust and promising approach. Important work on this topic has also been carried out by Betti et al. (2001; 2011).

In this case study we will present a proof-of-concept using a network of GNSS receivers to determine significance of the movement recorded on the vertical axis. All measures by sensors have a budget of residual errors, and each error function can be estimated and used in a model to calculate significance. This is typical in statistical analysis, and literature provides us with several methods. In the following chapter, we present and discuss the Bayesian approach used to analyse a time series of vertical displacement measures carried out in a GNSS network with ten vertices. The objective is to assess significance of each measure testing different models that represent the characteristics of the phenomenon under investigation, thus allowing better discrimination with respect to classical statistical inference.

2 Study area

The area which was tested is called Rovina di Cancìa, located in the Dolomites region (Northeast Italy –Fig. 1). It includes a basin whose main channel origins at the feet of Salvella Fork (2500 m a.s.l.) in the municipality of Borca di Cadore (Fig. 2), 15 km far from Cortina d'Ampezzo, and ends in a retaining basin systems (low deposition area) at 1005 m a.s.l.. The channel intersects a flat area at lower altitude (1344 m a.s.l.) which was specifically built to divert and slow down debris flow. Phenomena of landslide and of debris flows are present at this site. The latter are triggered just downstream a cyclopean boulder (Fig. 3) where runoff entrain large quantities of solid material and debris flow can form. For more detailed discussion on the site, see Gregoretti & Dalla Fontana, (2008)

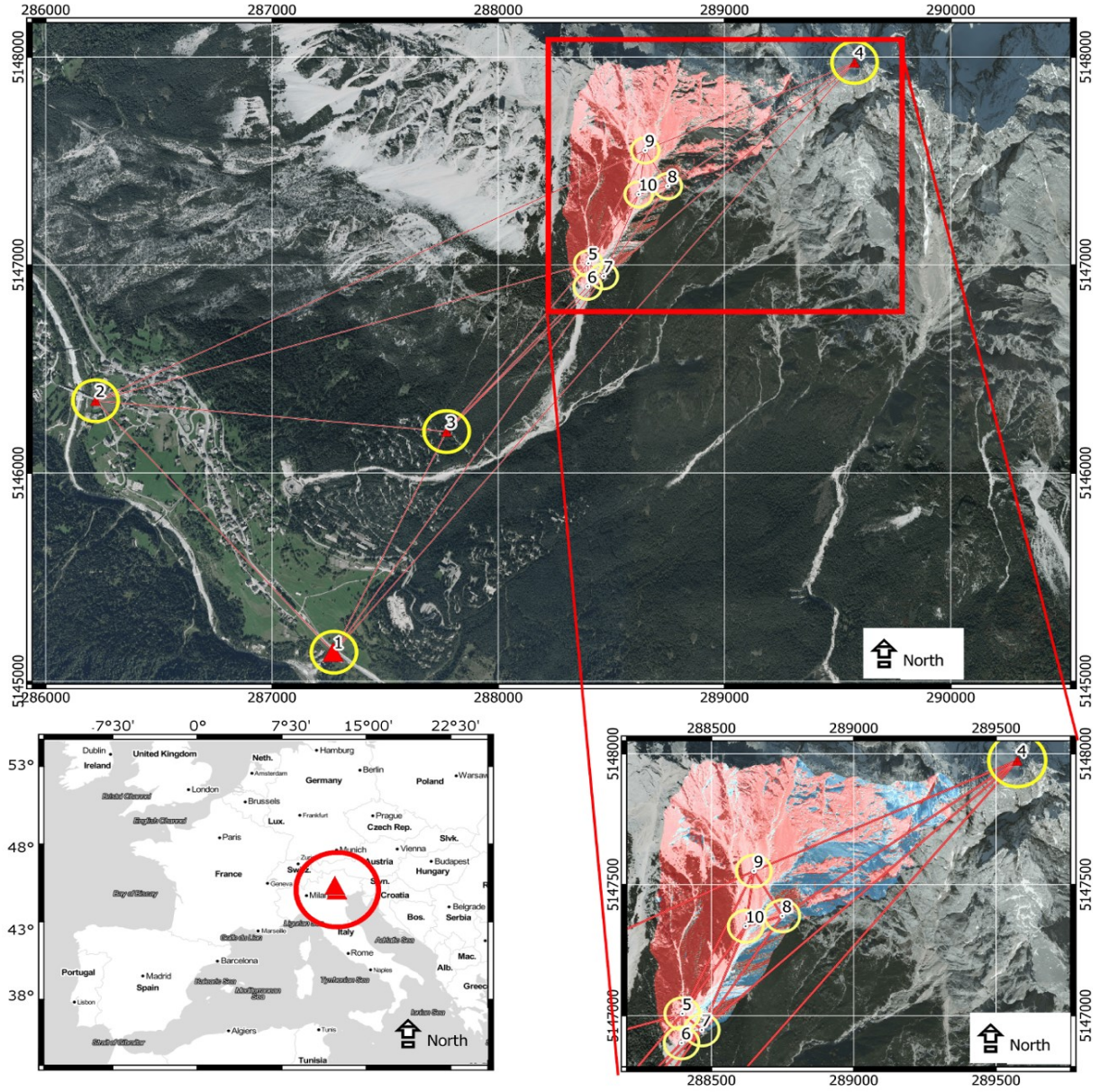

Figure 1 The GNSS control network

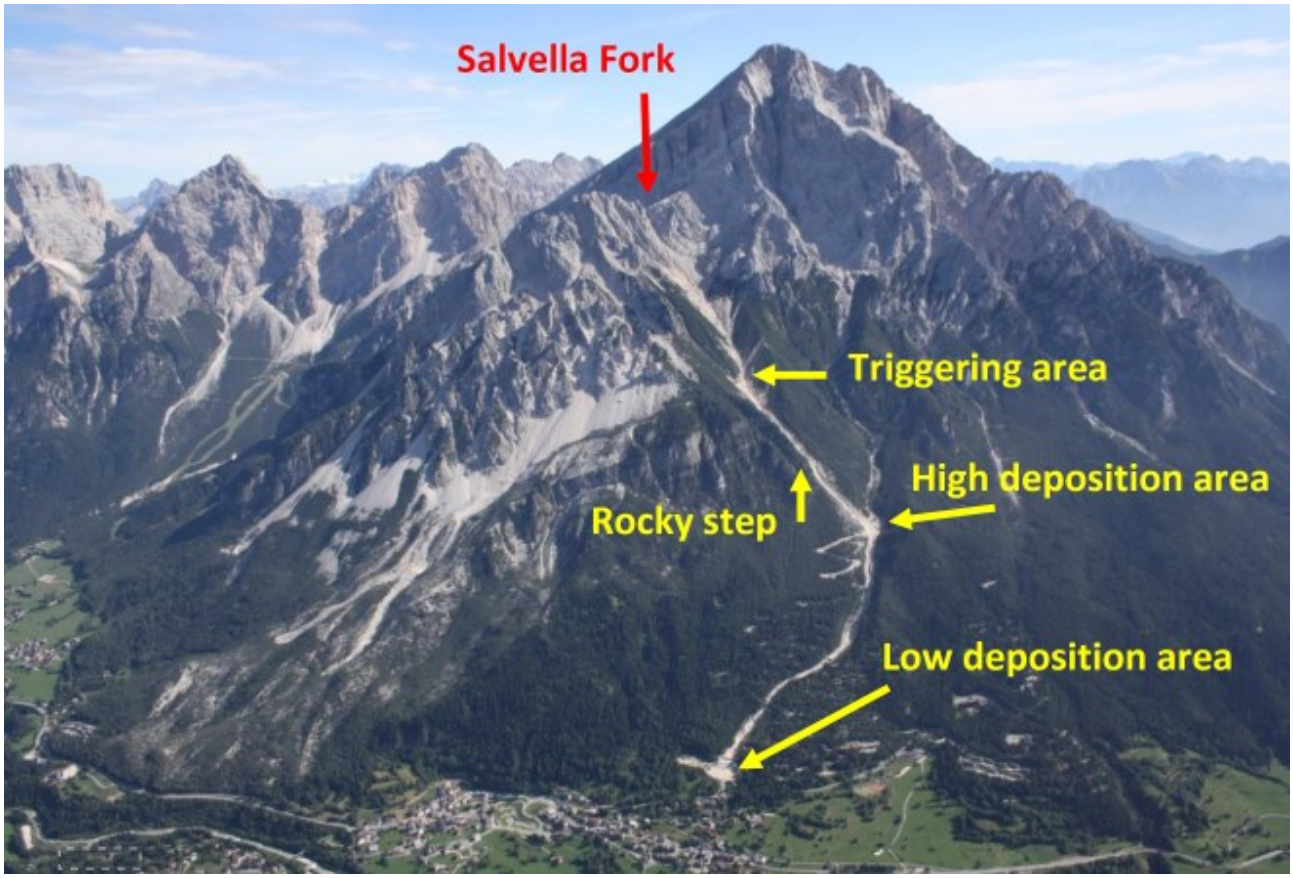

Figure 2 Study area 'Ravina di Cancìa' with the two main hydrological basins source: Ortofoto 2008 Regione Veneto mapped over a digital terrain model.

Figure 3 Details of the study site with loose gravel and surfacing rocks.

3 Materials and methods

3.1 The GNSS control network

A GNSS control network (CN) was created around the landslide area in order to determine small surface movements. The CN consists of ten points, four of which (1-4) are considered stable and are positioned at a distance from the landslide (**Errore. L'origine riferimento non è stata trovata.**), whereas the remaining 6 points (5-10) are positioned near the landslide body. The fixed points were defined using the Italian Geodetic network from the Istituto Geografico Militare (IGM 2014) which

has monumented several control points in the region. With classical topography (total station) we defined the fixed points were the GNSS receivers were then positioned.

The location of the set of the control points to monitor was detected using orthophotos and a LiDAR-derived digital terrain model (DTM) from an aerial survey carried out in 2003. The DTM was used to take into account the terrain morphology, logistics and safety (slopes steepness) issues, thus the overall accessibility. In order to determine the best set of candidate locations, several sky-plots were determined. Potential obstructions (e.g., due to vegetation, rocks and overall morphology) were derived from the LiDAR-derived DSM as well as from visual interpretation of the ortho-images. Five benchmarks were then selected and properly monumented in the field by cementing steel survey nails into the ground or into the rocks. This solution was adopted in order to easily recover the marks in subsequent surveys and to prevent possible displacements due to damage by local fauna or cattle. The length of all potential baselines of the resulting geodetic network ranges between 300 m and 5 km. Four survey campaigns have been performed between 2011 to 2013, with a six-month time interval: in May, after the snow-melting period, and in early October, before the winter season. Occupation time was set to 1 hour with a sampling rate of 10 seconds. For the data collection the following geodetic-grade GNSS receivers were employed: two Topcon HiPer Pro, a Leica Wild GNSS System 200 with SR299 antenna, and a Trimble 5700. A least squares free network adjustment was applied to each acquired dataset, using all available independent baselines. The computations were executed using TopconTools' software adopting the 'single base' approach. Preliminary loop closure analysis of the post-processed baselines showed all the time misclosures of a few millimetres, thus denoting the absence of any gross error in the observations. The resulting adjusted coordinates (N, E, h) of the ten control points are listed in table 1. Here the differences (ΔE, ΔN, Δh) have been computed with respect to the first survey epoch. Adjustment of the geodetic network yielded coordinate standard deviations at centimetre level.

Table 1. Coordinates of the points in the GNSS network with their residual error in terms of standard deviation after differential correction. Ep. = Epoch. Points 5-7 and 8-10 are respectively the lower and upper group of points near the landslide (**Errore. L'origine riferimento non è stata trovata.**)

	Ep.	E (m)	N (m)	h (m)	σE	σN	σh	ΔE (m)	ΔN (m)	Δh (m)
1	1	287273.634	5145139.688	990.154	0.03	0.03	0.08			
	2	287273.627	5145139.684	990.145	0.05	0.05	0.10	0.007	0.004	0.009
	3	287273.619	5145139.678	990.144	0.03	0.05	0.06	0.008	0.006	0.010
	4	287273.614	5145139.675	990.145	0.04	0.05	0.06	0.005	0.003	0.009
2	1	286220.336	5146347.164	968.639	0.03	0.04	0.10			
	2	286220.332	5146347.159	968.625	0.03	0.04	0.11	0.004	0.005	0.014
	3	286220.324	5146347.152	968.628	0.02	0.02	0.04	0.008	0.007	0.011
	4	286220.318	5146347.145	968.624	0.03	0.04	0.10	0.006	0.007	0.015
3	1	287771.711	5146198.934	1279.527	0.04	0.04	0.09			
	2	287771.705	5146198.930	1279.517	0.03	0.03	0.08	0.006	0.004	0.010
	3	287771.701	5146198.924	1279.512	0.05	0.02	0.08	0.004	0.006	0.015
	4	287771.694	5146198.921	1279.514	0.03	0.05	0.07	0.007	0.003	0.013
4	1	289574.834	5147974.169	3164.527	0.02	0.02	0.11			
	2	289574.830	5147974.161	3164.441	0.02	0.04	0.04	0.004	0.008	0.086
	3	289574.826	5147974.153	3164.449	0.02	0.05	0.07	0.004	0.008	0.078
	4	289574.821	5147974.150	3164.429	0.02	0.05	0.07	0.005	0.003	0.098
5	1	288398.021	5147007.454	1746.699	0.04	0.03	0.08			
	2	288398.014	5147007.431	1746.600	0.04	0.02	0.08	0.007	0.023	0.099
	3	288398.008	5147007.417	1746.599	0.04	0.05	0.05	0.006	0.014	0.100
	4	288397.991	5147007.387	1746.627	0.05	0.02	0.04	0.017	0.03	0.072
6	1	288395.084	5146895.914	1674.800	0.03	0.05	0.09			
	2	288395.061	5146895.896	1674.715	0.02	0.03	0.11	0.023	0.018	0.085
	3	288395.055	5146895.885	1674.724	0.05	0.02	0.04	0.006	0.011	0.076
	4	288395.033	5146895.879	1674.722	0.05	0.05	0.11	0.022	0.006	0.078
7	1	288466.157	5146945.457	1740.800	0.02	0.03	0.10			
	2	288466.134	5146945.441	1740.703	0.03	0.03	0.09	0.023	0.016	0.097
	3	288466.112	5146945.412	1740.709	0.02	0.03	0.06	0.022	0.029	0.091
	4	288466.099	5146945.401	1740.711	0.02	0.05	0.04	0.013	0.011	0.089
8	1	288749.217	5147380.425	2042.012	0.05	0.04	0.03			
	2	288749.202	5147380.380	2041.859	0.04	0.05	0.03	0.015	0.045	0.153
	3	288749.154	5147380.346	2041.872	0.02	0.02	0.02	0.048	0.034	0.140
	4	288749.107	5147380.307	2041.887	0.03	0.03	0.04	0.047	0.039	0.125

9	1	288649.394	5147552.146	2107.801	0.04	0.05	0.04			
	2	288649.354	5147552.116	2107.681	0.03	0.03	0.04	0.040	0.030	0.120
	3	288649.339	5147552.094	2107.652	0.04	0.04	0.05	0.015	0.022	0.149
	4	288649.312	5147552.056	2107.615	0.04	0.04	0.02	0.027	0.038	0.186
10	1	288620.624	5147340.959	1959.589	0.03	0.02	0.03			
	2	288620.575	5147340.942	1959.480	0.02	0.04	0.05	0.049	0.017	0.109
	3	288620.565	5147340.918	1959.407	0.04	0.04	0.03	0.01	0.024	0.182
	4	288620.546	5147340.871	1959.443	0.05	0.03	0.04	0.019	0.047	0.146

3.2 Analysis of displacements with the Bayesian method.

The Bayesian method applied to test significance over differences – in our case difference in vertical point position between epochs – tests the likelihood of such difference given the prior model of expected residuals (i.e., height differences due to error budget of GNSS) of the measure. The general formulation of Bayes theorem states that if A and B are two stochastic variables, scalars or vectors, with known probability density functions, P(A) and pP(B), the relation between the joint probability densities P(A,B) = P(B,A), the conditional probability densities P(A | B) and P(B | A) and the single probability densities P(A) and P(B) is defined as:

$$P(A,B) = P(A \mid B)P(B) = P(B \mid A)P(A) \quad (1)$$

which can be written as:

$$P(A \mid B) = \frac{P(B,A)}{P(B)} = \frac{P(A,B)}{P(B)} = \frac{P(B \mid A)P(A)}{P(B)} \quad (2)$$

resulting in Bayes theorem:

$$P(A \mid B) = \frac{P(B \mid A)P(A)}{P(B)} \tag{3}$$

In other words the likelihood that the difference is explained by the error model. On a simplified schema, if A is the accuracy in terms of expected normal distribution of the differences due to measuring errors, and B is the real difference we test the likelihood that B if significantly above the expected difference due expected error frequency distribution.

The Bayesian approach allows identifying in advance the areas on the ground with statistically significant shifts. A drawback of traditional statistical methods is that they work well only when point displacements between different survey epochs are sufficiently large compared to the standard deviations of related coordinates. In such cases, coordinate differences of some points can be marked as potential displacements by the classical methods. Bayesian analysis can help to better discriminate these 'ambiguities,' see Sacerdote et al. (2010). Point shifts computed with respect to the first measurement epochs had the same order of magnitude as the residuals of the corresponding coordinates.

In order to evaluate whether the differences in vertical coordinates, with respect to the values at epoch 1, are more likely to be caused by a movement then to be due to random measurement errors, the Bayesian approach is more robust, see Betti et al. (2011). The test was limited to the one-dimensional case since the results of classical analysis did not show any doubt on the horizontal components of the geodetic network points. Thus, for each point P_j the shifts Δh between different measurement campaigns were taken into account:

$$(\Delta h)_{P_j} = \left(h_i - h_1\right)_{P_j} \qquad with \;\; i = 2,...,6 \;\; and \;\; j = 1,...,5 \tag{4}$$

In equation (4) h_i denotes the adjusted height of point P_j at surveying epoch t_i, while h_1 is the adjusted height of the same point at the first measurement epoch t_1, considered as reference value. Assuming that the shifts Δh have a normal distribution with unknown mean δh and known variance σ_h^2 (computed from network adjustment), for each control point P_j the shift Δh can be written as:

$$\Delta h = h_i - h_1 = \delta h + \sigma_h \tag{5}$$

The mean δh is, in turn, a random variable following a normal distribution with mean μ and variance σ_0^2 which represents, in this analysis, the prior distribution of the Bayesian statistical inference. The parameters μ and σ_0^2 are the prior information whose values have to be somehow set in advance. Since the points 5 through 10 were placed close to the landslide area, it is reasonable to assume that the vertical displacements can be zero or negative (decrease in altitude). Therefore, considering a properly oriented axis, the following additional a-priori constraint has been set:

$$\delta h \geq 0$$

Considering the observables Δh as dependant on parameter δh, the Bayes formula becomes:

$$f(\delta h|\Delta h) = \frac{f(\Delta h|\delta h) \cdot f(\delta h)}{\int_{-\infty}^{+\infty} f(\Delta h|\delta h) \cdot f(\delta h) \cdot \delta h} \tag{6}$$

All the terms on the right of equation (above) can be explicitly calculated. The function f(δh) in this analysis denotes the a-priori probability distribution of parameters δh . This distribution follows a modified version of a normal distribution: along the negative semi-axis it is null, being the probability of the interval [-∞, 0] all concentrated in the origin, i.e., $P_0 \equiv P\{\delta h \leq 0\}$. Given this constraint, the probability distribution of δh becomes:

$$f(\delta h) = P_0\delta(\delta h) + \frac{\vartheta(\delta h)}{\sigma_0\sqrt{2\pi}} \cdot e^{-(\delta h-\mu)^2/2\sigma_0^2} \tag{7}$$

where (δh) is the unit step function (or Heaviside step function):

$$\vartheta(\delta h) = \begin{cases} 0 & for\ \delta h < 0 \\ 1 & for\ \delta h \geq 0 \end{cases} \tag{8}$$

and δ(δh) is the delta of Dirac function which is a generalized distribution that is zero everywhere except at zero.

The value of P_0 can be calculated by considering the normalization condition applied to the distribution probability f(δh). Indeed, from equation (9):

$$P_0\delta(\delta h) + \int_0^{+\infty} f(\delta h) \cdot d(\delta h) = 1 \tag{9}$$

it follows that

$$P_0 = \int_{-\infty}^{0} f(\delta h) \cdot d(\delta h) = \frac{1}{\sigma_0\sqrt{2\pi}} \cdot \int_{-\infty}^{0} e^{-(\delta h-\mu)^2/2\sigma_0^2} \cdot d(\delta h) \tag{10}$$

The integral on the right side of (10) can be solved using the error function (Zwillinger 2012) whose values are available in specific tables:

$$erf(z) = \int_{-\infty}^{z} \frac{1}{\sqrt{2\pi}} e^{-t^2/2} \cdot dt = \frac{1}{2} + \int_0^z \frac{1}{\sqrt{2\pi}} e^{-t^2/2} \cdot dt \tag{11}$$

This way, after a variable change, equation (7) becomes:

$$P_0 = \int_{-\infty}^{-\mu/\sigma_0} \frac{1}{\sqrt{2\pi}} e^{-t^2/2} \cdot dt = erf\left(-\frac{\mu}{\sigma_0}\right) \tag{12}$$

In equation (4) the function f(Δh|δh) can be regarded as the likelihood function L(Δh|δh) of variable Δh:

$$L(\Delta h|\delta h) = \frac{1}{\sigma_h \sqrt{2\pi}} \cdot e^{-(\Delta h - \delta h)^2 / 2\sigma_h^2} \tag{13}$$

The denominator of (6) is a normalization constant which can be numerically estimated. After some mathematical steps, the following formula is obtained:

$$K = A + B \tag{14}$$

with

$$A = \frac{P_0}{\sqrt{2\pi\sigma_h}} e^{-\Delta h^2 / 2\sigma_h^2} \tag{15}$$

and

$$B = \frac{\bar{\sigma} e^{\left(\frac{1^2}{2}\left[\frac{\Delta h^2}{\sigma_0^2} - \frac{m^2}{\bar{\sigma}^2}\right]\right)}}{\sqrt{2\pi}\sigma_h \sigma_0} \cdot \left[1 - erf\left(-\frac{m}{\bar{\sigma}}\right)\right] \tag{16}$$

Being all terms in equation (6) defined in explicit form, the Bayes formula can be now numerically evaluated as follows:

$$f(\delta h|\Delta h) = \frac{f(\Delta h|\delta h)\cdot f(\delta h)}{K} =$$
$$= \frac{\frac{1}{\sigma_h\sqrt{2\pi}}\cdot e^{-(\Delta h-\delta h)^2/2\sigma_h^2}\cdot\left(P_0\delta(\delta h)+\frac{\vartheta(\delta h)}{\sigma_0\sqrt{2\pi}}\cdot e^{-(\delta h-\mu)^2/2\sigma_0^2}\right)}{A+B} \tag{17}$$

The benefit of using the two quantities A and B becomes clear by evaluating the probability that significant (δh ≥ 0) or not significant (δh = 0) vertical displacements have occurred between 2011 and 2013. Indeed, this operation is turned into the calculation of the following simple ratios:

$$P(\delta h > 0|\Delta h) = \int_{-\infty}^{+\infty} P(\delta h|\Delta h)\cdot d(\delta h) = \frac{B}{A+B} \tag{18}$$

$$P(\delta h = 0|\Delta h) = \frac{1}{A+B}\cdot\frac{P_0}{\sqrt{2\pi\sigma_h}}\cdot e^{-\Delta h^2/2\sigma_h^2} = \frac{A}{A+B} \tag{19}$$

The significance analysis of displacements through the Bayesian approach is thus reduced to a comparison between the two quantities (18) and (19). A probabilistic analysis can be therefore performed instead of classical statistical testing. The result of the comparison allows to assess which of the two alternatives (significant or not significant shift) is more likely to be occurred.

While in classical statistical analysis a decision rule based on a confidence level (e.g., α=5%) in the Bayesian statistical analysis a different approach was adopted, as shown in Table 2.

Table 2. Criteria threshold for the Bayesian statistical analysis.

$P(\delta h > 0 \mid \Delta h)$	Interpretation
< 0.475	Point displacement is not significant $\rightarrow P(\delta h = 0 \mid \Delta h) > 0.525$
> 0.525	Point displacement is significant $\rightarrow P(\delta h = 0 \mid \Delta h) < 0.475$
$0.475 \div 0.525$	No assessment can be made about the significance of the displacement

Three tests were then carried out with different settings for the prior values of parameters μ and σ_0. For each test the probabilities $P(\delta h > 0|\Delta h)$ were calculated, assuming as reference for the comparisons the adjusted heights of the network points derived from the first measurement epoch. Although the classical analysis had highlighted some 'ambiguities' just for points P4 and P5, the Bayesian approach was applied to all the control points.

Finally to compare with classical statistics we applied a z-score comparison using the residuals of the corrections for the network:

$$Z = \frac{\Delta h}{\sqrt{\sigma_{v_1}^2 + \sigma_{v_2}^2}} \tag{20}$$

where $\sigma_{v_1}^2$ and $\sigma_{v_2}^2$ are known as they have been calculated by the least squares network adjustment at the two surveying epochs t_1 and t_2 and Δh is the difference in height. In order to statistically check the significance of the network point displacements, computed within the surveys, the null hypothesis tested was that no significant displacements occurred between two measurement epochs.

4 Results and discussion

Test results are illustrated in Table 3, where three different parameters for Bayesian data *prior* for each point in the control network are tested (A – C) and a column with the z-test scores are reported. Values which are above the threshold, and therefore significant, are in boldface. In the third Bayesian

test, the value of the parameter μ was set equal to the mean shift Δh for each point P*j*. The data prior (μ, σ_0) were set according to accumulated experience and knowledge about the landslide, derived from previous surveys. The first four points are not reported as they resulted in very low values, as expected, and we will focus on the points near the landslide body.

We can see from the data in boldface that the upper group of points (point 8, 9 and 10) have proven to be significantly shifting downwards. With a classical statistical test only two points, 8 and 9, and only in one case for each of the three compared height differences, show that the recorded values can be considered as genuine shifts and not as false positives due to residuals of the measures. The application of the Bayes approach gave results which included also point 10 as significant. It also included more than one epoch of survey for all three points as significant with respect to the first measure (t1). Historically it is known that there is a downward shift of that part of the basin, and our results are compatible with such information.

Table 3. Results of Bayesian analysis respectively with (A) $\mu = 0.040$ m, $\sigma_0 = 0.02$ m, (B) $\mu = 0.050$ m, $\sigma_0 = 0.05$ m and (C) μ = variable, $\sigma_0 = 0.08$ m.

Point	**Epoch**	**Δh (m)**	**A**	**B**	**C**	**z-score**
5	t2 - t1	-0.092	0.175	0.169	0.150	1.029
	t3 - t1	-0.1	0.210	0.123	0.062	1.060
	t4 - t1	-0.1	0.260	0.174	0.101	1.118
6	t2 - t1	-0.083	0.231	0.210	0.112	0.781
	t3 - t1	-0.095	0.213	0.207	0.170	1.062
	t4 - t1	-0.071	0.201	0.145	0.101	0.753
7	t2 - t1	-0.076	0.198	0.125	0.115	0.760
	t3 - t1	-0.079	0.274	0.180	0.168	0.837
	t4 - t1	-0.075	0.396	0.299	0.239	0.663
8	t2 - t1	-0.104	0.143	0.137	0.094	1.217
	t3 - t1	-0.187	**1.062**	**0.969**	**0.871**	**1.982**

	t4 - t1	-0.101	0.450	0.428	0.415	1.071
9	t2 - t1	-0.168	**0.963**	**0.894**	**0.823**	**2.037**
	t3 - t1	-0.114	**0.590**	**0.589**	0.320	1.334
	t4 - t1	-0.138	**0.527**	0.352	0.150	1.673
10	t2 - t1	-0.136	**0.709**	**0.638**	**0.619**	1.592
	t3 - t1	-0.119	**0.618**	**0.585**	**0.537**	1.393
	t4 - t1	-0.154	0.295	0.204	0.124	1.722

The variation of the data *prior* shows that the method is robust, giving coherent results and pushing to the same conclusions. Point 9 seems particularly sensible to the test, and we can see from Figure 1 that it is the point with higher altitude of the group; this suggests a relationship with the position along the main axis of the basin. It is an hypothesis which can be tested by adding points to the network and applying this approach to a larger network, or to another one positioned differently.

The application of the Bayes approach can also be used inversely, to prove that a control network is stable over time, and therefore that it can be used as control points for stationing other instruments which might be used for change detection and/or landslide monitoring using remote sensing techniques that were mentioned in the introduction. In our study case it was used to define points with significant vertical downward shift.

Traditional methods work well when coordinate differences between survey epochs are large enough, with respect to the residuals from error budget of the network adjustment, to remove any doubts on the cause of such difference. The Bayesian approach is not to be considered as a substitute to classical statistical testing, but as an integration, which can reliably give a more in-depth information clearing doubts in the case of border-line values. This can be done without having to increase the sample size, i.e., more surveys, as in the case of classical statistics, thus decreasing costs. The Bayesian approach works well when the movements have a preferred directionality; this might not be the case in many applications, so the phenomenon has to be interpreted beforehand and then a decision taken on which approach will work best.

5 References

Barbarella M, Fiani M, Lugli A (2013) Landslide monitoring using multitemporal terrestrial laser scanning for ground displacement analysis. *Geomatics, Natural Hazards and Risk*, 21 pages, available online at doi:10.1080/19475705.2013.863808.

Barbarella M, Fiani M, Lugli A (2013) Multi-temporal terrestrial laser scanning survey of a landslide. In: Scaioni M (Ed.) 'Modern Technologies for Landslide Investigation and Prediction,' Springer, Berlin (Germany).

Betti B, Biagi L, Crespi M, Riguzzi F (1999) GPS sensitivity analysis applied to non-permanent deformation control networks. *Journal of Geodesy* 73, 158–167, doi:10.1007/s001900050231.

Betti B, Cazzaniga NE, Tornatore V (2011) Deformation Assessment Considering an A Priori Functional Model in a Bayesian Framework. *Journal of Surveying Engineering* 137: 113–119, doi:10.1061/(ASCE)SU.1943-5428.0000052.

Betti B, Sansò F, Crespi M (2001) Deformation Detection According to a Bayesian Approach. In: Benciolini B (Ed.), Proc. 'IV Hotine-Marussi Symposium on Mathematical Geodesy,' *Int. Association of Geodesy Symposia*, Vol. 122, Springer, Berlin (Germany), pp. 83–88, doi:10.1007/978-3-642-56677-6_12.

Bitelli G, Dubbini M, Zanutta A (2004) Terrestrial laser scanning and digital photogrammetry techniques to monitor landslide bodies. *The International Archives of the Photogrammetry, Remote Sensing and Spatial Information Sciences* 38(7B).

Borghi A, Cannizzaro L, Vitti A (2012) Advanced Techniques for Discontinuity Detection in GNSS Coordinate Time-Series. An Italian Case Study. In: Kenyon S et al. (Ed.'s) 'Geodesy for Planet Earth,' *Int. Association of Geodesy Symposia*, Vol. 136, Springer, Berlin (Germany), pp. 627–634, doi:10.1007/978-3-642-20338-1_77.

Cina A, Piras M (2014). Performance of low-cost GNSS receiver for landslides monitoring: test and results. *Geomatics, Natural Hazards and Risk*, 18 pages, doi:10.1080/19475705.2014.889046.

Crosetto M, Monserrat O, Luzi G, Cuevas-González M, Devanthéry N (2014). Discontinuous GBSAR deformation monitoring. *ISPRS Journal of Photogrammetry and Remote Sensing* 93: 136–141, doi:10.1016/j.isprsjprs.2014.04.002.

Dowman I (2004) Integration of LiDAR and IFSAR for mapping. *The International Archives of the Photogrammetry, Remote Sensing and Spatial Information Sciences* 35(2), 11 pages.

Farina P, ColomboD, Fumagalli A, Marks F, Moretti S (2006) Permanent Scatterers for landslide investigations: outcomes from the ESA-SLAM project. *Engineering Geology* 88(3-4): 200–217, doi:10.1016/j.enggeo.2006.09.007.

Forlani G, Roncella R, Diotri F (2013) Production of high-resolution digital terrain models in mountain regions to support risk assessment. *Geomatics, Natural Hazards and Risk*, 19 pages, available online at doi:10.1080/19475705.2013.862746.

Frangioni S, Bianchini S, Moretti S (2014) Landslide inventory updating by means of Persistent Scatterer Interferometry (PSI): the Setta basin (Italy) case study. *Geomatics, Natural Hazards and Risk*, 20 pages, available online at doi:10.1080/19475705.2013.866985.

Gregoretti C, Dalla Fontana G (2008) The triggering of debris flow due to channel-bed failure in some alpine headwater basins of the Dolomites: Analyses of critical runoff. *Hydrological Processes* 22: 2248–2263, doi:10.1002/hyp.6821.

Hofmann-Wellenhof B, Lichtenegger H, Wasle E (2007) *GNSS - Global Navigation Satellite Systems: GPS, GLONASS, Galileo, and more*. Springer, Berlin (Germany), 516 pages.

IGM (2014) Rete Geodetica Nazionale. Available online at http://www.igmi.org/geodetica/ (last access on 10th July 2014).

Jaboyedoff M, Oppikofer T, Abellán A, Derron MH, Loye A, Metzger R, Pedrazzini A (2012) Use of LIDAR in landslide investigations: A review. *Natural Hazards* 61: 1-24, doi:10.1007/s11069-010-9634-2.

Koch K (2007) *Introduction to Bayesian Statistics*. Springer, Berlin (Germany).

Lingua A, Piatti D, Rinaudo F (2007) Remote Monitoring Of A Landslide Using an Integration of Gb-Insar and Lidar Techniques. *The International Archives of the Photogrammetry, Remote Sensing and Spatial Information Sciences* 37(B1): 361–366.

Manfré LA, Hirata E, Silva JB, Shinohara EJ, Giannotti MA, Larocca APC, Quintanilha JA (2012) An Analysis of Geospatial Technologies for Risk and Natural Disaster Management. *ISPRS International Journal of Geo-Information* 1(3): 166–185, doi:10.3390/ijgi1020166.

Monserrat O, Crosetto M, Luzi G (2014) A review of ground-based SAR interferometry for deformation measurement. *ISPRS Journal of Photogrammetry and Remote Sensing* 93: 40–48, doi:10.1016/j.isprsjprs.2014.04.001.

Pirotti F, Guarnieri A, Vettore A (2013) Vegetation filtering of waveform terrestrial laser scanner data for DTM production. *Applied Geomatics* 5(4): 311–322, doi:10.1007/s12518-013-0119-3.

Previtali M, Barazzetti L, Scaioni M (2014) Accurate 3D surface measurement of mountain slopes through a fully automated imaged-based technique. Earth Science Informatics 7: 109–122.

Refice A, Bovenga F, Wasowski J, Guerriero L (2000) Use of InSAR data for landslide monitoring: a case study from southern Italy. In: Proc. IGARSS 2000, Honolulu (HI, U.S.A.), 24-28 July 2000, Vol. 6, pp. 2504-2506, doi:10.1109/IGARSS.2000.859621.

Remondino F, Spera MG, Nocerino E, Menna F, Nez F (2014) State of the art in high density image matching. *The Photogrammetric Record* 29(146): 144–166.

Sacerdote F, Cazzaniga NE, Tornatore V (2010) Some considerations on significance analysis for deformation detection via frequentist and Bayesian tests. *Journal of Geodesy* 84: 233–242, doi:10.1007/s00190-009-0360-z.

Scaioni M, Feng T, Barazzetti L, Previtali M, Lu P, Qiao G, Wu H, Chen W, Tong X, Wang W, Li R (2014) Some applications of 2-D and 3-D photogrammetry during laboratory experiments for hydrogeological risk assessment. *Geomatics, Natural Hazards and Risk*, pages 24, available online at doi:10.1080/19475705.2014.885090.

Scaioni M, Feng T, Barazzetti L, Previtali, Roncella R (2014) Close-Range Photogrammetric Techniques for Deformation Measurement: Applications to Landslides. In: Scaioni M (Ed.) 'Modern Technologies for Landslide Investigation and Prediction,' Springer, Berlin (Germany).

Wang G, Soler T (2012) OPUS for Horizontal Subcentimeter-Accuracy Landslide Monitoring: Case Study in the Puerto Rico and Virgin Islands Region. *Journal of Surveying Engineering* 138(3): 143–153, doi:10.1061/(ASCE)SU.1943-5428.0000079.

Ye X, Kaufmann H, Guo XF (2004) Landslide Monitoring in the Three Gorges Area Using D-INSAR and Corner Reflectors. *Photogrammetric Engineering & Remote Sensing* 70: 1167–1172, doi:10.14358/PERS.70.10.1167.

Zwillinger D (2012) *CRC Standard Mathematical Tables*.